

MISMATCH INDUCED OSCILLATIONS OF SPACE CHARGE DOMINATED BEAMS IN A UNIFORM FOCUSING CHANNEL *

H. Higaki, S. Fujimoto, K. Fukata, K. Ito, M. Kuriki, H. Okamoto, and J. Aoki[†]

AdSM, Hiroshima Univ., 1-3-1 Kagamiyama, Higashi-Hiroshima, Hiroshima 739-8530, Japan

[†]Graduate School of Science, Osaka Univ., 1-1 Machikaneyama, Toyonaka, Osaka 560-0043, Japan

Abstract

A solenoid trap with a beam imaging system was employed to study the mismatch induced oscillations of a space charge dominated beams experimentally. It was observed that a spheroidal Gaussian beam with a density $n \sim 1.5 \times 10^8 \text{ cm}^{-3}$ and a local tune depression $\eta \sim 0.5$ could produce a large halo with an induced mismatch. Associated with the induced mismatch, the oscillations of the beam were also detected.

INTRODUCTION

Space charge effects due to the strong Coulomb interactions expected in high intensity accelerator beams result in undesirable beam degradation and radio-activation of the vacuum tubes through halo formations. Various space charge effects have been studied intensively with particle simulations [1, 2, 3, 4]. This is partly because the analytical formulation of the nonlinear evolution in high intensity beams is not possible in general cases. And the systematic study of space charge effects with the real accelerators is not feasible. Although the development of computation environment is outstanding, some approximations are still necessary so far.

Thus, it was proposed to use solenoid traps and linear Paul traps for investigating some properties of space charge dominated beams [5, 6, 7]. The key idea is that the charged particles (a plasma) in these traps are physically equivalent with beams in a FODO lattice.

Some experimental results were reported with the use of Paul traps [8, 9, 10, 11, 12, 13, 14, 15]. Here, a solenoid trap with a beam imaging system composed of a charge coupled device (CCD) camera and a phosphor screen (PS) was employed to study the mismatch induced oscillations of a space charge dominated beams.

THEORETICAL BACKGROUND

When charged particles (mass : m , charge : e) are confined with an infinitely long uniform magnetic field B in z direction, the Hamiltonian H_{sol} of a test particle, which

describes the motion in $x - y$ plane, becomes as follow.

$$H_{sol} = \frac{1}{2m} \left[\left(p_x + \frac{eBy}{2} \right)^2 + \left(p_y + \frac{eBx}{2} \right)^2 \right] + e\phi_{sc}$$

Here, ϕ_{sc} denotes the electric potential due to the space charge. When the system is observed in the rotating frame of reference around the z -axis (with the angular rotation frequency of $eB/2m$), the Hamiltonian is transformed to \tilde{H}_{sol} below.

$$\tilde{H}_{sol} = \frac{\tilde{p}_x^2 + \tilde{p}_y^2}{2} + \frac{1}{2}K_3(\tilde{x}^2 + \tilde{y}^2) + \frac{e}{mc^2}\tilde{\phi}_{sc} \quad (1)$$

The energy and momentum are normalized by mc^2 and mc , respectively and $K_3 = (eB/2mc)^2$. The quantities with tilda mean that these are observed in the rotating frame.

Since the Hamiltonian H_{beam} of a test particle in a periodic focusing channel can be approximated with

$$H_{beam} \approx \frac{p_x^2 + p_y^2}{2} + \frac{1}{2}K_1(z)(x^2 - y^2) + \frac{e}{p_0\beta_0c\gamma_0^2}\phi_{sc},$$

it is seen that there is a correspondence between two systems. Under the smooth focusing approximation of the periodic focusing channel, both systems are physically equivalent each other.

Assuming the Kapchinsky-Vladimirsky distribution for the charged particles, of the circular cross section with the radius a and the density n , the self field potential $\tilde{\phi}_{sc} = -\frac{en}{4\epsilon_0}(\tilde{x}^2 + \tilde{y}^2)$ can be substituted into eq.(1) to give

$$\tilde{H}_{sol} = \frac{\tilde{p}_x^2 + \tilde{p}_y^2}{2} + \frac{1}{2} \left(K_3 - \frac{K_s}{a^2} \right) (\tilde{x}^2 + \tilde{y}^2) \quad (2)$$

with $K_s = \frac{\pi a^2 n e^2}{2\pi\epsilon_0 m c^2}$. And the the radius a satisfies the envelop equation given by

$$a'' + K_3 a - K_s/a - \epsilon^2/a^3 = 0$$

with the beam emittance ϵ . Then, the space-charge limit is achieved when $K_3 - K_s/a^2 = 0$ and given by $n_{lim} = \frac{\epsilon_0 B^2}{2m}$. Also, the bare tune σ_0 , space-charge depressed tune σ , and the tune depression η of the solenoid system are described as below.

$$\sigma_0 = \frac{eB}{2mc}, \quad \sigma = \sqrt{K_3 - \frac{K_s}{a^2}}, \quad \eta = \frac{\sigma}{\sigma_0} = \sqrt{1 - \frac{n}{n_{lim}}}$$

Although the above formulation is valid for an infinitely long plasma column, it is also applicable for a uniform density spheroidal plasma confined in a harmonic potential [16].

05 Beam Dynamics and Electromagnetic Fields

D04 High Intensity in Linear Accelerators - Incoherent Instabilities, Space Char

* This work is partly supported by a Grant-in-Aid for Scientific Research from the Ministry of Education, Culture, Sports, Science and Technology (No. 20540483) and the 2008 Hiroshima University Fujii Research Promotion Fund. Promotion of collaborative research program : Support universities research and educational programs in promotion of accelerator science.

EXPERIMENTAL SETUP

A schematic of the experimental setup is shown in Fig.1(a). Fourteen solenoids are aligned along the axis of symmetry to provide the uniform axial magnetic field $B \sim 62.5$ G with the constant current of 20 A. The field limits the maximum density $n_{lim} \sim 1.9 \times 10^8$ cm⁻³. The vacuum chamber contains 45 ring electrodes with the inner diameter of 7 cm, which are also aligned along the axis of symmetry. Each ring electrode is located every 1.6 cm in axial direction. These ring electrodes can be also used to excite or detect axial oscillations of charged particles. This solenoid trap is quite flexible for applying various electric potential. Here, the harmonic potential $\phi_{ex} \propto (r^2 - 2z^2)$ is used to confine a spheroidal Gaussian beam.

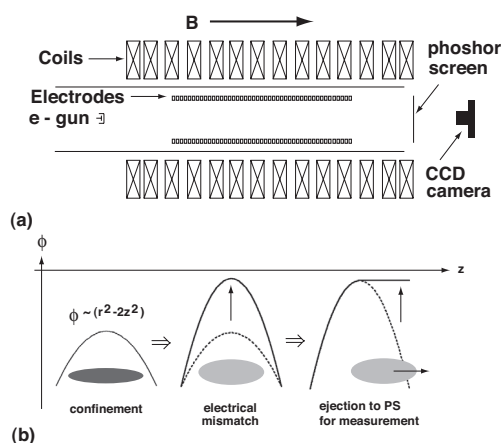


Figure 1: (a) A schematic of the multi-ring electrode trap in a uniform magnetic field. (b) Electrons are confined in a harmonic potential. Then, the potential depth is changed quickly to induce electrical mismatch and the profile is measured with the phospor screen.

A typical experimental procedure is as follow. The electrostatic potentials $V_1 \sim -53$ V, $V_i = -40$ V, and $V_2 = -80$ V are applied to ring electrodes at first as shown schematically in Fig.1(b). Among 45 electrodes, 27 electrodes near the electron gun were used to apply V_1 and 15 electrodes near PS were for V_2 . The rest of only 3 electrodes in between were used for applying V_i . Then, electrons were injected for ~ 500 μ sec with the energy of ~ 60 eV and V_1 was made -80 V to start a confinement. The applied external potential produced the harmonic potential $\phi_{ex} \propto (r^2 - 2z^2)$ near the axis of symmetry. It is known theoretically that a uniform density spheroid of charged particles can be a rigid rotor equilibrium state in the harmonic potential. When a mismatch was applied, V_i was changed to $V_f = 0$ V within 2μ sec. The oscillations of the electrons were detected by the electronic signals excited on a electrode. This is similar to observing Schottky signals in accelerators. Then, 20 μ sec later, V_2 was grounded to measure the radial density distribution and total electron number N_e with the PS.

Phosphor (P20) with the thickness of 15μ m and the effective diameter of 75 mm is mounted on a glass plate and

is aluminum coated (500 Å in thickness), which is biased to +8 kV for measurement. A grounded mesh was placed in front of PS to make the acceleration field almost parallel to the magnetic field. To obtain the images from PS when electrons are dumped, a progressive scan CCD camera (480×640 pixel, 10 bit, mono-chrome) was employed. Typically 100 images were accumulated for a profile measurement to improve the signal to noise ratio.

EXPERIMENTAL RESULTS

Shown in Fig.2 is an example of an equilibrium electron density profile in the trap, which is calculated [17] with the radial density distribution measured after 40 μ s confinement (Fig.3(a)). It is confirmed that the maximum density is about $n_{max} \sim 1.74 \times 10^8$ cm⁻³, which corresponds to the local tune depression of $\eta \sim 0.5$.

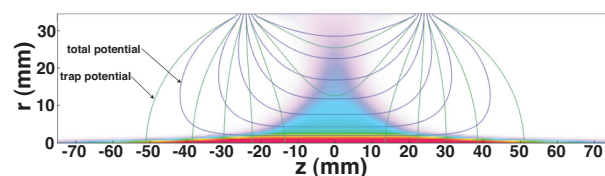


Figure 2: A density distribution of the confined electron plasma calculated with the measured radial density profile. The maximum density becomes 1.74×10^8 cm⁻³.

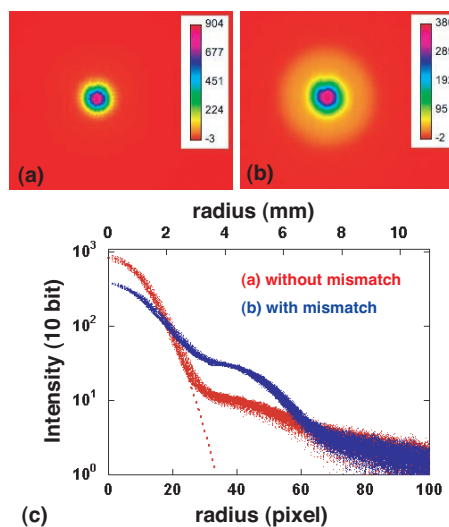


Figure 3: (a) An image (200×250 pixels) of extracted electron beam with $N_e \sim 9 \times 10^7$ without mismatch. (b) The mismatch was applied for the electrons in (a) with $V_f = 0$ V. It is clearly seen that some electrons were ejected in radial direction. (c) The radial distributions of measured intensity in logarithmic scale.

Figure 3(a) shows 100 shots averaged radial density profile without induced mismatch. On the other hand, in Fig.3(b), the effective mismatch ($\Delta V = 40$ V) was induced

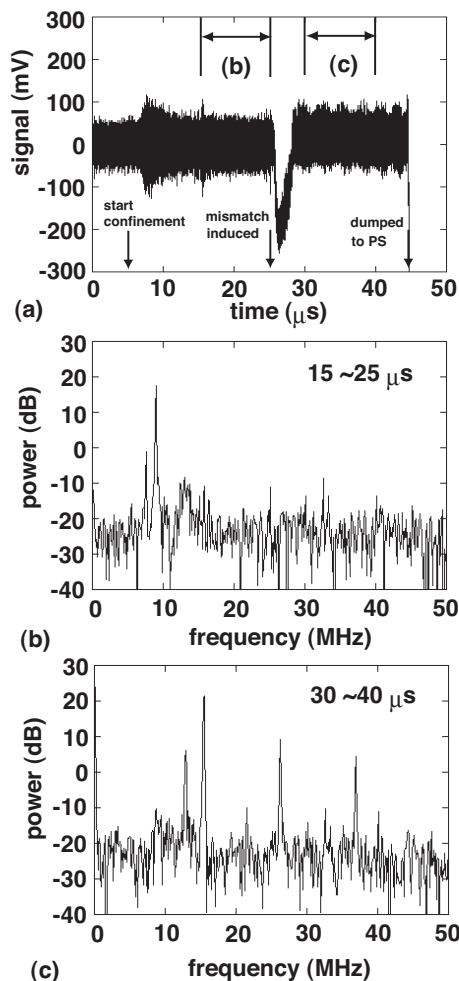


Figure 4: (a) A signal measured with a ring electrode as a function of time. (b) The FFT spectrum before the induced mismatch (15 to 25 μs). (c) The FFT spectrum after the mismatch (30 to 40 μs). Coherent axial oscillations were excited associated with the mismatch.

20 μs after the beginning of the confinement and the electrons were dumped 20 μs after the mismatch. In both figures, the color graduations are normalized to their peaks. Here, one pixel corresponds to 0.11 mm and the unit intensity corresponds to about 150 electrons per pixel squared or 1.2×10^6 electrons per cm^2 .

Also, shown in Fig.3(c) are the radial distributions of intensity as a function of radius up to 100 pixels from the beam center. The dashed line is a Gaussian fitting for the initial beam core (red points). It is seen that there are halo components at the radius larger than 30 pixels. Eventhough the initial profile has a small amount of halo, by comparing with the beam profile after the induced mismatch (blue points), it is clearly seen that a large amount of halo is created between 30 to 60 pixel.

It was experimentally confirmed that a beam with the higher density (smaller η) and/or the larger mismatch resulted in the larger halo. Here, attentions are paid for the oscillations of beams associated with the mismatch. In

Fig.4(a), the signal measured with a ring electrode is plotted as a function of time. The confinement started at 5 μs , the mismatch induced at 25 μs and the electrons were dumped to PS at 45 μs . Shown in Fig.4 (b) and (c) are the Fast Fourier Transformed (FFT) power spectra before (15 to 25 μs) and after (30 to 40 μs) the mismatch. It is clearly seen that two coherent axial oscillations were excited associated with the mismatch. At the moment, it is not clear if these oscillations enhance the production of halo or not. The details should be investigated more in the future experiments.

In summary, coherent axial oscillations of a confined charged particle beam were observed associated with the mismatch. Non-neutral plasmas confined in a uniform magnetic field can be used for the systematic investigation of space charge dominated beams under the smooth focusing approximation.

REFERENCES

- [1] R. L. Gluckstern, W.-H. Cheng, S. S. Kurennoy, and H. Ye : Phys. Rev. E **54** (1996) 6788.
- [2] H. Okamoto and M. Ikegami : Phys. Rev. E **174** (1997) 4694.
- [3] R. L. Gluckstern, A. V. Fedotov, S. Kurennoy, and R. Ryne : Phys. Rev. E **58** (1998) 4977.
- [4] A. V. Fedotov, R. L. Gluckstern, S. Kurennoy, and R. Ryne : Phys. Rev. ST Accel. Beams **2**, 014201 (1999).
- [5] H. Okamoto and H. Tanaka : Nucl. Instr. Meth. A **437** (1999) 178.
- [6] R. C. Davidson, H. Qin, and G. Shvets : Phys. Plasmas **7**, (2000) 1020.
- [7] H. Okamoto, Y. Wada, and R. Takai : Nucl. Instr. Meth. A **485** (2002) 244.
- [8] E. P. Gilson, R. C. Davidson, P. C. Efthimion, and R. Majeski : Phys. Rev. Lett. **92**, 155002 (2004).
- [9] R. Takai, H. Enokizono, K. Ito, Y. Mizuno, K. Okabe, and H. Okamoto : Jpn. J. Appl. Phys. **45** (2006) 5332.
- [10] M. Chung, E. P. Gilson, M. Dorf, R. C. Davidson, P. C. Efthimion, and R. Majeski : Phys. Rev. ST Accel. Beams **10** (2007) 014202.
- [11] K. Ito, K. Nakayama, S. Ohtsubo, H. Higaki, and H. Okamoto : Jpn. J. Appl. Phys. **47** (2008) 8017.
- [12] R. Takai, H. Enokizono, K. Ito, Y. Mizuno, K. Okabe, and H. Okamoto : J. Phys. Soc. Jpn. **76** (2007) 014802.
- [13] H. Higaki, K. Ito, R. Takai, K. Nakayama, W. Saiki, K. Izawa, and H. Okamoto : Hyperfine Interactions **174** (2007) 77.
- [14] M. Chung, E. P. Gilson, R. C. Davidson, P. C. Efthimion, and R. Majeski : Phys. Rev. Lett. **102** (2009) 145003.
- [15] N. Kjergaard, K. Mølhave, and M. Drewsen : Phys. Rev. E **66** (2002) 015401.
- [16] J. J. Bollinger, D. J. Heinzen, F. L. Moore, W. M. Itano, and D. J. Wineland : Phys. Rev. A, **48** (1993) 525.
- [17] J. Aoki, Y. Kiwamoto, and Y. Kawai : Phys. Plasmas, **13** (2006) 112019.